

# Propene Oligomerization using Alkali Metal- and Nickel-Exchanged Mesoporous Aluminosilicate Catalysts

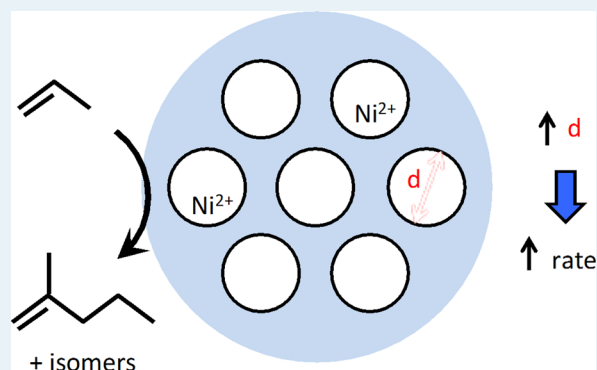
Anton N. Mlinar, Sankaranarayanapillai Shylesh, Otto C. Ho, and Alexis T. Bell\*

Department of Chemical and Biomolecular Engineering, University of California, Berkeley, California 94720-1462, United States

## Supporting Information

**ABSTRACT:** A series of alkali metal- and nickel-exchanged Al-MCM-41 catalysts were prepared via aqueous ion exchange and then investigated for gas-phase oligomerization of propene at 453 K and near ambient pressures. All catalysts were active and produced oligomers with >98% selectivity. The highest activities per  $\text{Ni}^{2+}$  cation were observed when the cations were highly dispersed as a consequence of either lowering the Ni loading for a fixed MCM-41 Si/Al ratio or by decreasing the concentration of exchangeable sites within the material by increasing the MCM-41 Si/Al ratio at a fixed Ni loading. The identity of the alkali metal cation had no significant effect on the catalytic activity or degree of dimer branching, except for the sample containing  $\text{Cs}^+$  cations, where the decreased pore volume resulted in a lower catalyst activity and slightly more linear dimer products. Comparison of Ni-MCM-41 prepared with and without  $\text{Na}^+$  cations showed that a higher yield of oligomers could be achieved when  $\text{Na}^+$  cations are present because of partial removal of strong Brønsted acid sites. For the same reaction conditions, Ni-Na-MCM-41 was more than twice as active as smaller-pored Ni-Na-X zeolites, demonstrating that the activity of  $\text{Ni}^{2+}$  cations increases with the increasing free volume near the site. This effect of free volume on the activity of  $\text{Ni}^{2+}$  cations was further confirmed by comparing the activities of Ni-Na-X, Ni-Na-MCM-41, Ni-Na-MCM-48, and Ni-Na-SBA-15 with respect to pore size.

**KEYWORDS:** oligomerization, propene, MCM-41, nickel, alkali metal



## 1. INTRODUCTION

The oligomerization of low molecular weight ( $\text{C}_2$ – $\text{C}_4$ ) olefins to produce higher molecular weight oligomers suitable as lubricants, detergents, and liquid fuels can be catalyzed by Brønsted acidic zeolites and nickel-containing heterogeneous catalysts.<sup>1–3</sup> Of particular note are nickel aluminosilicates, which exhibit particularly high selectivity to oligomers.<sup>4–7</sup> While the activity of these catalysts has been attributed to isolated  $\text{Ni}^{2+}$  cations, little is known about how the support and other cations present in the catalysts affect the activity of  $\text{Ni}^{2+}$  cations, weight distribution of oligomers, and distribution of stereoisomers at a given molecular weight. Toward developing such an understanding, we have recently shown that changing the alkali metal or alkaline earth cocation, M, in Ni-M-X zeolites has a large effect on the catalyst activity and dimer isomer distribution for propene oligomerization.<sup>8</sup> These effects are ascribed to the presence of alkali metal and alkaline earth cations altering the free volume around a Ni cation within a supercage, with increased catalytic activity and dimer branching observed for catalysts with larger supercage free volume. This conclusion suggests that even higher oligomerization rates might be achieved by introducing Ni cations into a larger-pored support, such as mesoporous aluminosilicates.

Ni-containing MCM-41 materials were first reported to be active catalysts for ethene dimerization over 15 years ago;<sup>9</sup>

however, it is only recently that the reactivity and properties of these materials have been studied in more detail. Studies for ethene oligomerization conducted using Ni-exchanged Al-MCM-41 in a slurry reactor<sup>10,11</sup> have shown that such catalysts are stable and have a high selectivity to oligomers. It was proposed that the ethene oligomerization activity in these studies arises from the presence of both Brønsted acidic and exchanged Ni sites. By contrast, a more recent study has demonstrated that siliceous Ni-exchanged MCM-41 is active for ethene oligomerization, suggesting that Brønsted acid sites are not required and that the activity is instead caused solely by three-coordinated  $\text{Ni}^{2+}$  cations.<sup>12</sup> The latter finding is consistent with our own studies of propene oligomerization over Ni-Na-X zeolites,<sup>13</sup> which demonstrated that catalytic activity is due solely to isolated  $\text{Ni}^{2+}$  sites. This more recent work suggests that Brønsted acid sites are not required to produce an active oligomerization catalyst and that poisoning these sites in Ni-MCM-41 with alkali metal cations, in a manner similar to Ni-M-X zeolites, could lead to more active olefin oligomerization catalysts with increased product tunability.

**Received:** September 5, 2013

**Revised:** November 2, 2013

**Published:** December 10, 2013

To examine this proposition, a series of alkali metal- and nickel-exchanged Al-MCM-41 materials were synthesized and explored as gas-phase propene oligomerization catalysts. Exchange of alkali metal and nickel cations into the MCM-41 material resulted in catalysts that were both active and selective for propene oligomerization and produced oligomers in a higher yield than the catalyst without alkali metal cations. The dispersion of the Ni<sup>2+</sup> cations within the catalyst, controlled by either varying the nickel loading or density of exchangeable Al sites, influenced the catalyst activity with the highest rate per Ni site being achieved at the lowest catalyst Ni density. The identity of the noncatalytic alkali metal did not alter the catalytic activity or selectivity greatly, with the exception of Cs<sup>+</sup>, where a decrease in activity was observed. Comparing the propene oligomerization activity of Ni-Na-MCM-41 to that of Ni-Na-X revealed that the larger-pored mesoporous materials are more active than smaller-pored zeolites under the same reaction conditions. Examination of other Ni-exchanged MCM-41, MCM-48, and SBA-15 materials further highlights this correlation between space and catalytic activity with the highest activity per Ni site being observed for the largest-pored sample, SBA-15.

## 2. METHODS

**2.1. Catalyst Preparation.** Al-MCM-41 was synthesized via a procedure similar to that used to produce vanadium-substituted MCM-41,<sup>14</sup> except that aluminum nitrate was substituted in place of vanadyl sulfate. In all syntheses, the molar ratio was 0.33 NaOH (EMD, >99.0%): 0.5 C<sub>16</sub>TABr (Acros, >99%): 1 SiO<sub>2</sub> (tetraethyl orthosilicate, Sigma-Aldrich, 98%): *x* Al(NO<sub>3</sub>)<sub>3</sub> (Alfa Aesar, 98.0–102%, nonahydrate): 108 H<sub>2</sub>O (Millipore filtered), where *x* was varied in the range 0.023–0.10 to produce Al-MCM-41 materials with Si/Al molar ratios of 10–40. The synthesis mixture was refluxed for 48 h in a round-bottomed flask equipped with a water-cooled condenser and a Teflon-coated stir bar. The resulting Al-MCM-41 was filtered, rinsed with Millipore purified water and ethanol, and allowed to dry before being calcined in a vertical tube furnace at 823 K for 24 h in flowing air.

Following calcination, alkali metal cations were exchanged into the Al-MCM-41 materials by mixing 2.5 g of Al-MCM-41 with 100 mL of 1 M LiNO<sub>3</sub> (Sigma, >99.0%), NaNO<sub>3</sub> (Sigma-Aldrich, >99.0%), KNO<sub>3</sub> (Mallinckrodt Baker), or CsNO<sub>3</sub> (Sigma-Aldrich, 99%) prepared using Millipore-filtered water. The mixture was stirred in a round-bottomed flask for 6 h at ambient temperature before it was filtered and rinsed with Millipore water to remove residual nitrates. The resulting cation exchanged Al-MCM-41 material was then placed in a vacuum oven at 363 K overnight to remove excess water and stored in a gastight amber bottle until further use.

Nickel was introduced into Al-MCM-41 by ion-exchanging 1 g of Al-MCM-41 with 50 mL of 5 mM Ni(NO<sub>3</sub>)<sub>2</sub> (Sigma-Aldrich, 99.999%, hexahydrate) solution. The exchange was performed in the same apparatus as that described above with the mixture being stirred at room temperature for 6 h before being filtered and rinsed with Millipore water. The resulting Ni-MCM-41 was then placed in a quartz boat in a horizontal quartz tube furnace where it was heated to 773 at 2 K min<sup>-1</sup> in air (Praxair, zero-grade) flowing at 100 cm<sup>3</sup> min<sup>-1</sup> and held at 773 K for 3 h to remove water and nitrate groups still left in the catalyst. Following this procedure, the sample was removed from the furnace, stored in a gastight vial, and placed in a desiccator to limit the readsorption of atmospheric moisture.

Additional Al-MCM-41 materials with various pore sizes were synthesized by varying the aliphatic tail length of the surfactant template from C<sub>12</sub> to C<sub>18</sub> and following the procedure described above. Al-MCM-48 and Al-SBA-15 were synthesized by modifying previously published procedures for the formation of siliceous MCM-48<sup>15</sup> and SBA-15<sup>16</sup> structures so as to incorporate aluminum nitrate into the synthesis gel. Full details of these syntheses procedures are provided in the Supporting Information.

**2.2. Catalyst Characterization.** The Si, Al, Ni, and alkali metal (M) content of the catalysts was determined by ICP-OES elemental analyses performed by Galbraith Laboratories (Knoxville, TN). Catalyst surface areas, pore volumes, and average pore sizes were measured by N<sub>2</sub> (Praxair, 99.999%) adsorption carried out in a Micromeritics Gemini VII BET instrument. Samples were outgassed overnight at 393 K under vacuum to remove residual water prior to measuring Brunauer–Emmett–Teller (BET) isotherms. Low angle X-ray diffraction (XRD) diffractograms were collected using a Bruker Advance D8 powder X-ray diffractometer over the range of 2θ = 1.25–10°. Temperature-programmed reduction (TPR) experiments were performed using a Micromeritics AutoChem II 2920 chemisorption instrument with 50 mL min<sup>-1</sup> of 10% H<sub>2</sub> diluted in Ar (Praxair, certified standard) and heating the catalyst to 1073 at 10 K min<sup>-1</sup>. The baseline of the TPR spectrum of Ni-Na-MCM-41 was adjusted using the TPR spectrum of Na-MCM-41.

**2.3. Measurement of Reaction Rates.** The catalytic activity of Ni-MCM-41 was performed in a 0.5 in. outer-diameter, stainless steel reactor.<sup>8</sup> The reactor was loaded with 0.050 g of the Ni-MCM-41 diluted with 0.450 g Silicycle silica (average pore diameter = 150 Å; surface area = 300 m<sup>2</sup> g<sup>-1</sup>) to minimize pressure drop and channeling through the catalyst bed. Each catalyst was calcined in situ at 773 K for 3 h (2 K min<sup>-1</sup> ramp rate) in 1 bar air flowing at 100 cm<sup>3</sup> min<sup>-1</sup> to remove any adsorbed water prior to the start of each experiment. The reactor was then flushed with 100 cm<sup>3</sup> min<sup>-1</sup> of helium (Praxair, 99.999%) for 5 min before introducing 30 cm<sup>3</sup> min<sup>-1</sup> of propene (Praxair, 99.9%) and increasing the pressure to reaction conditions. Reaction products were analyzed using an Agilent 7890A gas chromatograph equipped with two in-line gas-sampling valves, two columns, and two flame ionization detectors. The first 30 m HP-Plot Q column was used to separate products based on carbon number alone, while the second 100 m detailed hydrocarbon analysis (DHA) column (Wasson-ECE) was used with the Envantage Dragon DHA software package to identify individual dimer isomers.

## 3. RESULTS AND DISCUSSION

**3.1. Catalyst Characterization.** The BET surface areas, BJH (Barrett–Joyner–Halenda) pore volumes, and average pore sizes for the unexchanged H-Al-MCM-41 material as well as for all of the Ni-M-MCM-41 materials, where M is the alkali metal cation, are presented in Table 1. The as-synthesized H-Al-MCM-41 has a surface area of 1151 cm<sup>2</sup> g<sup>-1</sup> and an average pore diameter of 24.7 Å, consistent with the formation of MCM-41 using the synthesis procedure described above.<sup>14</sup> Confirmation of the successful synthesis of Al-MCM-41 was obtained from low-angle XRD diffractograms, which exhibited the 100 and 110 peaks characteristic of MCM-41<sup>14</sup> (see Supporting Information).

**Table 1. Elemental Analysis, BET Surface Area, BJH Pore Volume, and Average Pore Size for the Parent H-MCM-41 Material and Each Ni-M-MCM-41 (Si/Al = 20) Catalyst**

sample	elemental analysis [wt%]		surface area [m <sup>2</sup> g <sup>-1</sup> ]	pore volume [cm <sup>3</sup> g <sup>-1</sup> ]	pore size [Å]
	Ni	M			
H-MCM-41			1151	0.654	24.7
Ni-Li-MCM-41	1.04	0.01	1015	0.614	23.0
Ni-Na-MCM-41	0.96	0.10	1000	0.624	23.7
Ni-K-MCM-41	0.94	0.36	1011	0.647	23.4
Ni-Cs-MCM-41	0.57	2.43	821	0.519	24.5

Table 1 also shows that the pore size is maintained after ion exchange with the alkali metal and nickel cations, although the pore volume decreases slightly after the aqueous exchanges. The observed decrease in pore volume is consistent with what has been reported previously for MCM-41 treated in water<sup>17</sup> and is attributed to partial structure collapse of the mesoporous network. The identity of the alkali metal cation did not affect the pore size or the pore volume of the MCM-41 except for the sample containing Cs<sup>+</sup> cations, which had a smaller pore volume than the other materials. The low pore volume of this sample could be due to either the larger Cs<sup>+</sup> cations taking up more space in the pores of the MCM-41 or to further structural collapse upon exchange of cesium into MCM-41 than was observed for other alkali metal cations.

The content of Ni and alkali metal cations (M) are listed in Table 1 for each of the Ni-M-MCM-41 (Si/Al = 20) samples. The data demonstrate that Ni exchange does not lead to a complete loss of M from the sample and that, with the exception of Cs<sup>+</sup>, the identity of the alkali metal cation does not affect the final Ni loading. The TPR spectrum of Ni-Na-MCM-41 after calcination (see Supporting Information) exhibits only one high-temperature peak at approximately 1050 K. This observation is consistent with Ni<sup>2+</sup> cations being present as charge compensating cations, as shown in Figure 1, and is in

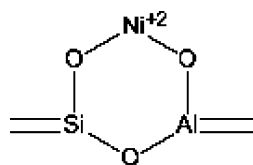


**Figure 1.** Illustration showing the nature of an exchanged Ni<sup>2+</sup> cation in the Ni-MCM-41 material after calcination in air at 773 K and before exposure to propene.

accordance with previous observations for Ni-exchanged zeolites<sup>13,18</sup> and Ni-exchanged MCM-41.<sup>10</sup> The absence of a peak in the range of 623–715 K, corresponding to the reduction of bulk NiO,<sup>8,10,18</sup> indicates that all of the Ni cations in Ni-Na-MCM-41 are present as isolated Ni<sup>2+</sup> cations in the as-prepared material.

The effect of Ni(NO<sub>3</sub>)<sub>2</sub> concentration in the exchange solution on the loading of Ni in Ni-Na-MCM-41 (Si/Al = 20) is shown in Figure 2. The data demonstrate that the Ni loading can be controlled by varying the concentration of Ni(NO<sub>3</sub>)<sub>2</sub> in the exchange solution; however, above a Ni(NO<sub>3</sub>)<sub>2</sub> concentration of 5 mM, the loading of Ni did not change significantly. The maximum Ni loading that could be achieved through the

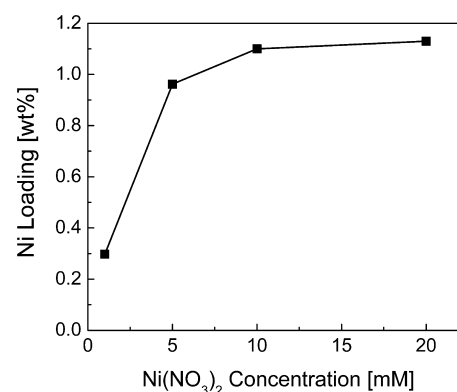


**Figure 2.** Ni loading in Ni-Na-MCM-41 (Si/Al = 20) as a function of the Ni(NO<sub>3</sub>)<sub>2</sub> exchange concentration.

aqueous ion exchange was determined to be approximately 1.15 wt %.

The Si/Al ratio of the Ni-Na-MCM-41 was examined by synthesizing a series of MCM-41 samples with nominal Si/Al ratios between 10 and 40. The actual Si/Al ratio and Ni loading after Ni exchange are presented in Table 2 for each sample.

**Table 2. Nominal and Actual Si/Al Ratio of MCM-41 When Varying the Aluminum Content in the Synthesis Gel As Well As the Ni Loading in the Corresponding Ni-Na-MCM-41 Materials**

nominal Si/Al	actual Si/Al	Ni [wt%]
10	12	1.07
15	16	0.81
20	19	0.96
40	37	0.74

Good agreement between the nominal and actual Si/Al ratios is observed, indicating that changing the aluminum content in the synthesis gel can change the Al content in the final material. Table 2 also shows that there is only a weak correlation between Ni loading and Si/Al ratio. In fact, the Ni loadings of these materials are similar over the range Si/Al = 10–20 with only the sample containing the least number of exchangeable Al sites, Si/Al = 40, having a lower Ni loading.

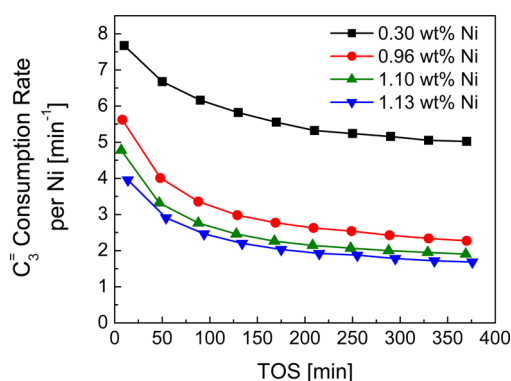
The properties of Ni-Na-MCM-41 prepared with various surfactants and those of Ni-Na-MCM-48 and Ni-Na-SBA-15 are presented in Table 3. Changing the length of the aliphatic tail in the template produced Ni-Al-MCM-41 samples with a range of pore sizes and surface areas, consistent with previous reports.<sup>14</sup> MCM-48 was prepared using the C<sub>16</sub>TABr template and formation of this structure was confirmed by the appearance of the characteristic 211 and 200 peaks in the low-angle XRD diffractogram<sup>15</sup> (see Supporting Information). After exchange with the Na<sup>+</sup> and Ni<sup>2+</sup> cations, the Ni-Na-MCM-48 was found to have a slightly smaller pore size and surface area than the Ni-Na-MCM-41 produced with the same surfactant; however, a surface area of 913 m<sup>2</sup> g<sup>-1</sup> and pore size of 20.5 Å still suggest retention of the MCM-48 structure. Al-substituted SBA-15 was found to have a pore size of 57.7 Å and a BJH pore volume of 0.830 cm<sup>3</sup> g<sup>-1</sup> after synthesis from the synthesis gel, consistent with the formation of the SBA-15 structure.<sup>16</sup> After Na<sup>+</sup> and Ni<sup>2+</sup> cation exchange, the pore size of the structure remained unchanged at 57.4 Å, but the pore volume decreased to 0.678 cm<sup>3</sup> g<sup>-1</sup>, similar to what was

**Table 3.** Ni Loadings, BET Surface Areas, BJH Pore Volumes, and Average Pore Sizes for Ni-Na-MCM-41, Ni-Na-MCM-48, and Ni-Na-SBA-15 Materials Synthesized with Different Pore Sizes

sample	template	Ni [wt%]	surface area [ $\text{m}^2 \text{g}^{-1}$ ]	pore volume [ $\text{cm}^3 \text{g}^{-1}$ ]	pore size [ $\text{\AA}$ ]
Ni-Na-MCM-41	$\text{C}_{12}\text{TABr}$	0.97	1109	0.311	20.3
Ni-Na-MCM-41	$\text{C}_{16}\text{TABr}$	0.96	1000	0.624	23.7
Ni-Na-MCM-41	$\text{C}_{18}\text{TABr}$	1.02	865	0.596	25.8
Ni-Na-MCM-48	$\text{C}_{16}\text{TABr}$	0.78	913	0.148	20.5
Ni-Na-SBA-15	P123 (MW = 5800)	0.06	719	0.678	57.4

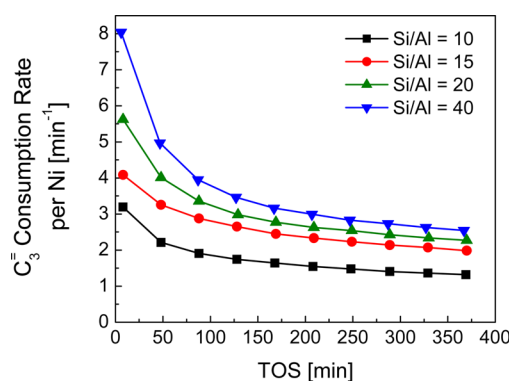
observed for MCM-41 after aqueous ion exchange. The resulting Ni-Na-SBA-15 was found to have a lower Ni loading than the MCM materials, likely because of the small number of sites available for Ni exchange caused by the low content of Al in the material (0.05 wt %).

**3.2. Effects of Ni Loading and Si/Al Ratio.** The effect of Ni loading on the activity of Ni-Na-MCM-41 (Si/Al = 20) for propene oligomerization was measured at 453 K and 1 bar propene pressure. The results of these experiments are shown in Figure 3. In agreement with the previous observations for

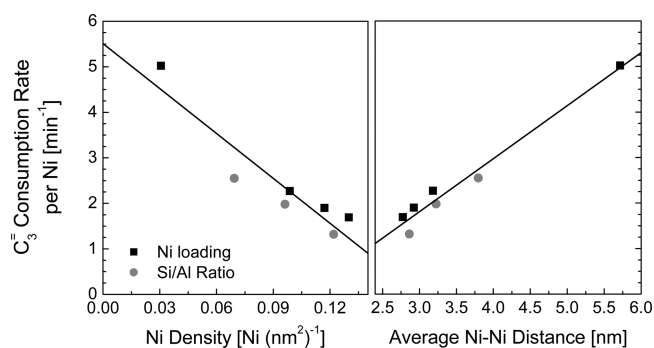
**Figure 3.** Time on stream activity of Ni-Na-MCM-41 (Si/Al = 20) for propene oligomerization as a function of the catalyst Ni loading.  $T = 453 \text{ K}$ ,  $P = 1 \text{ bar}$  propene,  $F = 30 \text{ cm}^3 \text{ min}^{-1}$  propene (STP).

ethene oligomerization,<sup>12</sup> the propene oligomerization activity per Ni cation was found to increase with decreasing Ni loading. It is also noted that all of the catalysts deactivated with time on stream and attempts at stabilizing the catalysts by increasing the temperature to 493 K for the first 120 min time on stream, shown to work for propene oligomerization in Ni-Na-X zeolites,<sup>13</sup> did not lead to catalyst stabilization. A possible cause for deactivation could be the relatively high yield of oligomers heavier than the dimer (discussed in Section 3.4) that cannot easily desorb from the catalyst and hence block active sites. This suggests that the increased catalyst activity at low Ni loadings may be caused by an increased stability of Ni sites, as long oligomers cannot block as many active sites if they are more highly dispersed on average at lower Ni loadings. It is also noted that while Ni-Na-MCM-41 loses activity with time on stream when used for gas-phase oligomerization, work with similar catalysts used for ethene oligomerization conducted in a slurry reactor show stable activity.<sup>10,11</sup> Therefore, it is conceivable that steady-state oligomerization of propene might be attainable when used in a liquid phase such as that in a slurry reactor.

Higher average dispersion of Ni within the support could also be achieved by increasing the Si/Al ratio, and thereby decreasing the volume density of exchangeable sites. Figure 4 shows this effect for a series of Ni-Na-MCM-41 materials with

**Figure 4.** Effect of Si/Al ratio in Ni-Na-MCM-41 on the propene oligomerization time on stream activity at 453 K, 1 bar propene pressure, and  $30 \text{ cm}^3 \text{ min}^{-1}$  propene flow rate (STP). Ni loading = 1.07, 0.81, 0.96, and 0.74 wt % for Si/Al = 10–40 respectively.

Si/Al ratios ranging from 10 to 40. In agreement with ethene oligomerization performed in a batch reactor,<sup>10</sup> an increase in Si/Al ratio was found to increase the catalyst activity for propene oligomerization per Ni site. All of the catalysts deactivated with time on stream, as was the case when varying the catalyst Ni loading; however, catalysts with fewer Ni sites per gram of catalyst were determined to remain the most active with time on stream. This again implies that an increase in catalyst activity per Ni site can be achieved by increasing the average distance between Ni sites within the catalyst. Figure 5

**Figure 5.** Propene oligomerization activity at approximately 375 min of time on stream ( $T = 453 \text{ K}$ ,  $P(\text{C}_3) = 1 \text{ bar}$ ,  $F(\text{C}_3) = 30 \text{ cm}^3 \text{ min}^{-1}$  at STP) as functions of Ni surface density and average distance between  $\text{Ni}^{2+}$  cations within Ni-Na-MCM-41 for nickel loadings spanning 0.3–1.13 wt % Ni and Si/Al ratios spanning 10–40.

further demonstrates this point. Here the rate of propene oligomerization measured after 375 min of time on stream is plotted against the average distance between Ni sites for Ni-Na-MCM-41 catalysts with various Ni loadings and Si/Al ratios. A strong correlation is observed between the average distance between  $\text{Ni}^{2+}$  cations in the support and the activity per  $\text{Ni}^{2+}$

cation indicating that dispersion of the active sites within MCM-41 has a significant effect on the specific activity of the Ni. Furthermore, the close agreement between the two sets of data indicate that the specific activity of Ni can be increased in a similar manner either by decreasing the Ni loading for a given Si/Al ratio or by increasing the Si/Al ratio of MCM-41 for a given Ni loading.

**3.3. Role of the Alkali Metal Cations.** As recently reported for propene oligomerization with alkali metal- and alkaline earth-exchanged Ni-X zeolites,<sup>8</sup> the identity of the noncatalytic cocation can affect both the catalyst activity and degree of dimer branching. To determine if the identity of the cocation affects the activity and product selectivity in Ni-MCM-41 catalysts as well, a series of alkali metal-exchanged Ni-MCM-41 (Si/Al = 20) materials was synthesized and examined for propene oligomerization. The results collected at 453 K and 1 bar propene pressure are shown in Figure 6. It is clear that all of

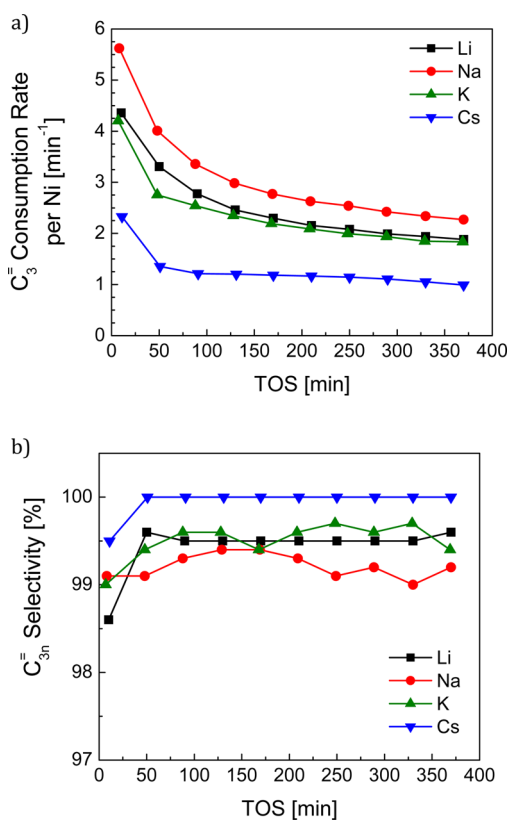


**Figure 6.** (a) Rate of propene consumption per total Ni and (b) oligomer selectivity as a function of time on stream for all Ni-M-MCM-41 (Si/Al = 20).  $T = 453$  K,  $P = 1$  bar,  $F = 30$  cm<sup>3</sup> min<sup>-1</sup> propene (STP).

the catalysts are active and >98.5% selective toward the formation of propene oligomers. In general, it was observed that the identity of the cation did not greatly alter the catalytic activity, with the exception of the sample containing Cs<sup>+</sup>, which was found to be the least active catalyst. The low activity of the Ni-Cs-MCM-41 is likely due to the decreased pore space in this catalyst (see Table 1), a point that is discussed further in Section 3.1.

Comparison of the activity of Ni-Na-MCM-41 to the material without alkali metal cations present shows that exchange of alkali metal cations into the catalyst increases the selectivity toward propene oligomers at short times on stream

where the activity of both materials is similar (see Supporting Information). The increased selectivity toward oligomers is consistent with at least partial exchange of strong Brønsted acid sites by alkali metal cations, since Brønsted acid protons have been shown to be active for secondary reactions, such as oligomer cracking.<sup>1–3</sup> At longer times on stream, the oligomer selectivity of both materials with and without alkali metal cations approaches 99% (see Supporting Information), and the activity of both materials decreases but at different rates—for the alkali metal-exchanged Ni-MCM-41 the propene conversion was 2.75% propene at 375 min TOS and for Ni-H-MCM-41 the propene conversion was 2% after the same time on stream. The observed increase in activity of Ni-Na-MCM-41 relative to Ni-H-MCM-41 taken together with the increasing oligomer selectivity with time on stream suggest that the activity at longer times on stream comes mainly from Ni sites as the Brønsted acid sites, responsible for oligomer cracking, deactivate first. This conclusion is consistent with a previous study in which Ni-H-MCM-41 was used for ethene oligomerization.<sup>10</sup> In that study it was proposed that Ni sites deactivate more slowly than Brønsted acid sites. The removal of some Brønsted acid sites by alkali metal cation exchange could, therefore, lead to increased catalyst stability and cause an overall increase in catalyst activity at longer time on stream, consistent with what is observed experimentally.

As was previously reported for alkali metal- and alkaline earth-exchanged Ni-X zeolites, the identity of the noncatalytic cocation can also be used to tune the degree of dimer branching by varying the amount of space around the Ni site.<sup>8</sup> Figure 7 shows that the degree of dimer branching is nearly the

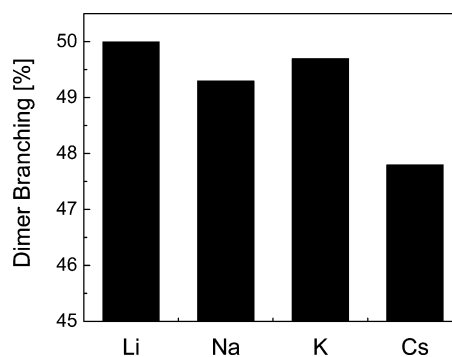


**Figure 7.** Degree of branching in the dimer product as a function of the noncatalytic cocation, M, for Ni-M-MCM-41 catalysts at 453 K, 1 bar propene pressure, 30 cm<sup>3</sup> min<sup>-1</sup> propene (STP), and approximately 150 min time on stream.

same for Ni-M-MCM-41 (Si/Al = 20) when M = Li, Na, or K, but decreases slightly when M = Cs. Since the pore volume is smallest for Ni-Cs-MCM-41, the observed trend is consistent with that found for Ni-M-X zeolites, for which it was found that a decrease in the space around the Ni site led to more linear products. This indicates that the amount of space around the active site can still influence the degree of oligomer branching in large pore aluminosilicate structures such as MCM-41 (pore diameter = 23 Å), although the effect is much less pronounced than it is in smaller-pored zeolites (supercage diameter = 11 Å).

**3.4. Comparison of Ni-Na-MCM-41 to Other Heterogeneous Ni Catalysts.** Figure 8 compares the propene oligomerization activity of Ni-Na-MCM-41 (Si/Al = 20) to that for Ni-exchanged Na-X (Si/Al = 1.2).<sup>13</sup> The Ni loading for both catalysts is 0.6 wt %, and the reaction conditions are

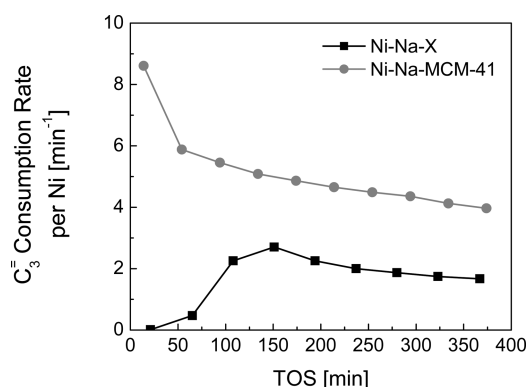


**Figure 8.** Comparison of time on stream propene oligomerization activity of Ni-Na-MCM-41 (Si/Al = 20) and 0.6 wt % Ni-exchanged Na-X zeolite, from ref 13 at 453 K, 5 bar propene pressure, and 30 cm<sup>3</sup> min<sup>-1</sup> propene at STP.

identical at 453 K and 5 bar propene pressure. Figure 8 shows that Ni-Na-MCM-41 is more active per Ni site than the Ni-Na-X zeolite. As was shown recently for alkali metal- and alkaline earth-exchanged Ni-X zeolites,<sup>8</sup> increasing the amount of space around the Ni site in the zeolite supercage leads to an increased propene oligomerization rate. Since MCM-41 has a much larger pore size than zeolite X, 24 Å as compared to 11 Å in the zeolite supercage, the propene oligomerization activity per Ni site should be larger in the MCM-41, in good agreement with the results shown in Figure 8.

Also observed in Figure 8, the time on stream activity of the Ni-Na-MCM-41 material is significantly different than that for the Ni-Na-X zeolite. The absence of the activation period in the Ni-Na-MCM-41 catalyst is expected as it was previously shown that this regime was due to migration of Ni<sup>2+</sup> cations from inaccessible hexagonal prisms of the zeolite to the supercages.<sup>13</sup> As the MCM-41 structure does not have positions outside of the pore where the Ni<sup>2+</sup> cations can reside, migration of the Ni<sup>2+</sup> cations is not necessary to activate the catalyst and therefore the activation period observed for the zeolite should not be observed for MCM-41. After the zeolite activation regime, both the Ni-Na-X and Ni-Na-MCM-41 catalysts deactivate; however, the Ni-Na-X material stabilizes after long times on stream.<sup>13</sup> Heating the Ni-Na-X catalyst to 493 K for the first 120 min of time on stream was found to increase the rates of catalyst activation and deactivation eventually leading to stable catalyst activities when cooled back to 453 K. As mentioned in Section 3.2, attempts using the same procedure for Ni-Na-MCM-41 did not lead to stabilization of the catalytic activity. This is likely due to differences in the deactivation mechanisms between the two catalysts. In the zeolite, the activity decreased hyperbolically with time on stream suggesting a two-site deactivation mechanism.<sup>13,19</sup> It was proposed that the deactivation pathway involved two nearby sites complexing together, leading to deactivation of both sites, and leaving only those sites that were well isolated to be active and stable. For the Ni-Na-MCM-41, the activity decreases exponentially with time on stream suggesting a different, one-site deactivation pathway. In this case, the deactivation is likely caused by the relatively high yield of longer oligomers, such as trimers, which constitute up to 14% of the total products produced with MCM-41 catalysts as compared to only 6% for the zeolite. These higher molecular weight oligomers would require higher temperatures to desorb and could coke up the

catalyst and block active sites once they are formed. This effect is not as prevalent in the Ni-Na-X zeolite since the activation energy for trimer formation was determined to be larger than that for dimer formation, suggesting that the sterics of the framework may make it more energetically unfavorable to form long oligomers.<sup>13</sup> With an increase in the pore size, however, the steric effects of the support would be diminished, minimizing this effect, and leading to both a higher oligomerization activity as well as an increased catalyst deactivation because of the increased rate of long oligomer growth in the Ni-MCM-41 materials.

Although the oligomerization activity did increase with increasing pore size, the degree of dimer branching did not change from 49% when changing from Ni-Na-X to the larger-pored Ni-Na-MCM-41 catalyst. This result is unexpected as increasing the free space in Ni-X zeolites using different alkali metal or alkaline earth cocations was determined to increase both the activity and degree of dimer branching.<sup>8</sup> We note that Ni-Na-MCM-41, which provides more space around the active site than Ni-Na-X, does not produce dimers with a higher degree of branching than those produced for Ni-Na-X, suggesting that the degree of dimer branching may be controlled by more than just spatial constraints. As seen in Figure 7 and discussed in Section 3.3, the identity of the cocation in the Ni-M-MCM-41 material has only a small effect on the degree of dimer branching, but not nearly as much as it does in Ni-M-X zeolites. Since the alkali metal cations are further apart on average in the more open-pored MCM-41 than in the zeolite, this difference in the degree of dimer branching between the two catalysts may suggest that the noncatalytic cocations need to be in close proximity to the active sites to influence the degree of dimer branching. Thus, it is possible the alkali metal cations provide both a steric and an electronic effect on the degree of dimer branching.

As previously reported for ethene oligomerization using Ni-Al-MCM-41 catalysts in the liquid phase,<sup>10</sup> increasing the pore size of the support beyond 24 Å can lead to further increases in catalytic activity. Therefore, a series of aluminosilicate supports with various pore sizes and topologies were synthesized and ion-exchanged with Na<sup>+</sup> and Ni<sup>2+</sup> cations to determine if the activity could be further increased for gas-phase propene oligomerization. Figure 9 shows the propene oligomerization activity of each of these materials after 400 min of time on

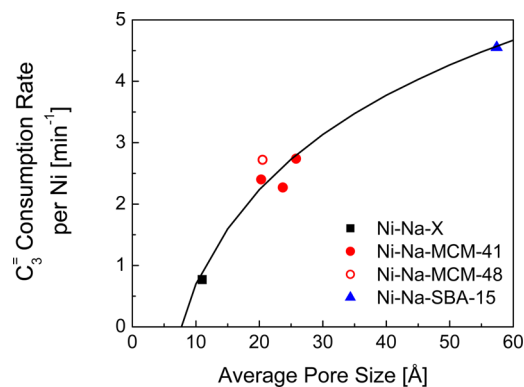


**Figure 9.** Relationship between the pore size of the support and the catalytic activity of Ni-Na-X, Ni-Na-MCM-41, Ni-Na-MCM-48, and Ni-Na-SBA-15 catalysts after approximately 400 min of time on stream.  $T = 453$  K,  $P = 1$  bar propene pressure,  $F = 30$  cm<sup>3</sup> min<sup>-1</sup> propene (STP) for all catalysts.

stream plotted as a function of the average support pore size. All catalysts exhibited greater than 99% selectivity to oligomers, which were composed of 49% branched dimers, 21% of which had terminal double bonds. As shown in Figure 9, there is a strong relationship between the catalytic activity and the pore size of the support, with the Ni-Na-SBA-15 exhibiting the highest catalyst activity. The increase in catalytic activity with increasing pore size agrees with what was previously reported for ethene oligomerization using Ni-Al-MCM-41 as catalysts;<sup>10</sup> however, the results contradict a more recent study using pure siliceous Ni-MCM-41 where it was found that smaller pores led to increased catalytic activity.<sup>12</sup> This difference may be due to the different bonding interactions between the Ni<sup>2+</sup> cations and the support for the two materials. In Ni-Al-MCM-41, the Al sites can provide exchangeable sites where Ni<sup>2+</sup> cations can anchor to the support, as shown in Figure 1, leading to the formation of an active Ni species similar to that found in zeolites. In the absence of Al, the Ni<sup>2+</sup> cations can only interact with silanol groups leading to the formation of a different active site that may have a dependence on the density of silanol groups on the surface, as discussed in ref 12.

Figure 9 also shows that the dimensionality of the pore system does not influence the catalytic activity significantly as the similarly pore sized three-dimensional MCM-48 and one-dimensional MCM-41 catalysts have similar activities. The curve drawn through the data in Figure 9 also shows that the effect of increasing pore size diminishes as the size of the pores becomes large. This suggests that the space around the Ni<sup>2+</sup> active site in smaller-pored structures, such as zeolites, would have the largest effect on catalyst activity, consistent with what has been observed for Ni-M-X catalysts.<sup>8</sup> Taken together, Figure 9 suggests that the space around the Ni<sup>2+</sup> site is the predominant factor governing catalyst activity and indicates that this parameter could be used to tune the activity of future Ni-based oligomerization catalysts.

#### 4. CONCLUSIONS

Ni-M-MCM-41 (M = Li, Na, K, Cs) catalysts were investigated for propene oligomerization at 453 K and near ambient pressure. All of the catalysts examined were active and selective for oligomerization. High activity per Ni cation was achieved by maintaining a high dispersion of the cations in the zeolite achieved by decreasing the Ni loading for a fixed Si/Al ratio of the support or by increasing the Si/Al ratio for a fixed Ni loading. The identity of the noncatalytic cation (M) had a small effect on the catalyst activity and oligomer selectivity. The only exception was for Ni-Cs-MCM-41, for which the smaller pore volume led to a decrease in catalyst activity. The propene oligomerization activity per Ni site of Ni-Na-MCM-41 was significantly higher than that of Ni-exchanged Na-X zeolite prepared with the same Ni loading and investigated under the same reaction conditions. Since MCM-41 has larger pores than the zeolite, this suggests that the increased space around the active Ni<sup>2+</sup> sites is responsible for their higher specific activity, a pattern previously reported for propene oligomerization with alkali metal- and alkaline earth-exchanged Ni-X zeolites. This conclusion is further supported by the data shown in Figure 9, which demonstrates a systematic increase in the propene oligomerization turnover frequency with increasing size of the pores in the support and independent of the pore connectivity.

#### ■ ASSOCIATED CONTENT

##### Supporting Information

Further details are given in three additional figures, Figures S1–S3. This material is available free of charge via the Internet at <http://pubs.acs.org>.

#### ■ AUTHOR INFORMATION

##### Corresponding Author

\*E-mail: [bell@cchem.berkeley.edu](mailto:bell@cchem.berkeley.edu). Phone: +1 510 642 1536. Fax +1 510 642 4778.

##### Notes

The authors declare no competing financial interest.

#### ■ ACKNOWLEDGMENTS

The authors would like to thank Sebastian Werner and Michael Nigra for help with the TPR measurements, Dr. Benjamin Keitz for help collecting the XRD measurements, and John Howell for his assistance in gathering some of the data. This work was supported by the XC<sup>2</sup> program funded by BP.

#### ■ REFERENCES

- (1) O'Connor, C. T.; Kojima, M. *Catal. Today* **1990**, *6*, 329–349.
- (2) Sanati, M.; Hörmell, C.; Järås, S. G. In *Catalysis*; Spivey, J. J., Ed.; The Royal Society of Chemistry: Cambridge, U.K., 1999; pp 236–287.
- (3) Corma, A.; Iborra, S. In *Catalysts for Fine Chemical Synthesis*; Derouane, E. G., Ed.; J. Wiley & Sons Ltd.: United Kingdom, 2006; Vol. 4, pp 125–140.
- (4) Wendt, G.; Fritsch, E.; Deininger, D.; Schöllner, R. *React. Kinet. Catal. Lett.* **1981**, *16*, 137–141.
- (5) Heveling, J.; Van der Beek, A.; De Pender, M. *Appl. Catal.* **1988**, *42*, 325–336.
- (6) Kiessling, D.; Froment, G. F. *Appl. Catal.* **1991**, *71*, 123–138.
- (7) Heveling, J.; Nicolaidis, C. P.; Scurrell, M. S. *Appl. Catal., A* **1998**, *173*, 1–9.
- (8) Mlinar, A. N.; Ho, O. C.; Bong, G. G.; Bell, A. T. *ChemCatChem* **2013**, *5*, 3139–3147.
- (9) Hartmann, M.; Pöppel, A.; Kevan, L. *J. Phys. Chem.* **1996**, *100*, 9906–9910.
- (10) Hulea, V.; Fajula, F. *J. Catal.* **2004**, *225*, 213–222.
- (11) Lallemand, M.; Finiels, A.; Fajula, F.; Hulea, V. *Chem. Eng. J.* **2011**, *172*, 1078–1082.
- (12) Tanaka, M.; Itadani, A.; Kuroda, Y.; Iwamoto, M. *J. Phys. Chem. C* **2012**, *116*, 5664–5672.
- (13) Mlinar, A. N.; Baur, G. B.; Bong, G. G.; Getsoian, A.; Bell, A. T. *J. Catal.* **2012**, *296*, 156–164.
- (14) Shylesh, S.; Singh, A. P. *J. Catal.* **2005**, *233*, 359–371.
- (15) Samuel, P. P.; Shylesh, S.; Singh, A. P. *J. Mol. Catal. A: Chem.* **2007**, *266*, 11–20.
- (16) Shylesh, S.; Singh, A. P. *J. Catal.* **2006**, *244*, 52–64.
- (17) Shylesh, S.; Samuel, P. P.; Singh, A. P. *Microporous Mesoporous Mater.* **2007**, *100*, 250–258.
- (18) Maia, A. J.; Louis, B.; Lam, Y. L.; Pereira, M. M. *J. Catal.* **2010**, *269*, 103–109.
- (19) Butt, J. B.; Petersen, E. E. In *Activation, Deactivation, and Poisoning of Catalysts*; Academic Press, Inc.: San Diego, CA, 1988; p 34.